JOURNAL OF MATERIALS SCIENCE: MATERIALS IN MEDICINE 13 (2002) 1193–1197

Synthesis of porous hydroxyapatites by combination of gelcasting and foams burn out methods

S. PADILLA, J. ROMÁN, M. VALLET-REGÍ*
Departamento de Química Inorgánica y Bioinorgánica. Facultad de Farmacia, Universidad Complutense de Madrid, 28040 Madrid, Spain
E-mail: vallet@farm.ucm.es

The biocompatibility and the osteoconductive behavior of hydroxyapatite (OHAp) ceramics are well established. Bioceramics made of OHAp are available in dense and porous form. Recently it has been proved that the volume of bone ingrowth at early times is primarily interconnectivity dependent. A new method for the obtention of porous OHAp ceramics that combine the in situ polymerization (gel casting method) and the foams burn out is proposed. Four polyurethane foams with different cells/cm were used. The foams were fully filled of an OHAp polymerizable suspension that after gelled produced very homogeneous and strong green bodies. After different thermal treatments the green bodies yield porous OHAp ceramics that were a replica of the foams used. Materials used in this work were studied by X-ray diffraction (XRD), X-ray fluorescence (XRF), scanning electron microscopy (SEM), N_2 adsorption isotherm, particle size distribution, and Hg porosimetry. Porous pieces of OHAp obtained are constituted by polyhedral-like particles (0.45–1.0 μm) that are surrounded by an interconnected network of pores. A bimodal distribution of the pores size between 30.8–58.6 and 1.0–1.2 μm has been observed. The size of the interconnected pores (30.8–58.6 μm) was controled as a function of the cells/cm of the foam while the volume of the small pores was modified as a function of the sintering time. The presence of pores could promote the bone ingrowth and also could be used to insert different drugs, which makes these porous pieces a potential candidate to be used as non-load-bearing bone implants and as drug delivery systems.

1. Introduction

Hydroxyapatite (OHAp) ceramics have been widely used as implant materials, mainly due to their close similarity in composition and high compatibility with nature bone [1–4]. Bioceramics made of OHAp are available in dense and porous form. Porous OHAp is more resorbable and more osteoconductive than dense OHAp, and it has been used as artificial bone graft material in many experimental and clinical trials [5, 6]. The formation of new bone depends greatly on the pore characteristics such as porosity, pore size, pore size distribution, and pore shape [7, 8]. It is suspected that the size of interconnection of the pores is the main limiting factor of osteoconduction rather than the size of the pores themselves [9]. In this sense, it has been reported that the volume of bone ingrowth at early times is primarily pore interconnectivity dependent [10]. Although a minimum pore size of 100–135 μm is generally considered acceptable for healthy bone ingrowth, active osteoconduction has been observed in porous OHAp with cylindrical pores with ∅ 50 μm [9] and in porous pieces with average of interpore connection of 40 μm [11].

In recent years, several methods have been proposed to obtain porous OHAp ceramics such as the inclusion of volatile or combustible substances that are lost during firing, hydrothermal exchange from corals, gel casting of foams and salt leaching [12–19]. One of the methods used consist in the coating of foam's skeleton with ceramic slurry that produces a replica of the network structure of the foam [9, 20, 21]. In the present paper the foam is fully filled of an OHAp polymerizable suspension that after gelled produces a very homogeneous cast body and very strong green bodies. After different thermal treatments the green bodies, previously prepared, yield a porous ceramic that is a replica of the foam and not of the skeleton. With this route, which is a combination of burn out of foams [9, 20, 21] and gel casting [22, 23] methods, it is possible to obtain pieces

* Author to whom all correspondence should be addressed.

of porous ceramics with a network of interconnected pores.

2. Materials and methods

2.1. OHAp preparation

OHAp was prepared by reaction of calcium hydroxide and orthophosphoric acid in aqueous solution. Reagent grade $Ca(OH)_2$ (Riedel-deHaën), H_3PO_4 (Merck), and deionized water were used. The reaction was carried out at 90 °C. The H_3PO_4 solution was slowly added to a $Ca(OH)_2$ suspension until the pH decreased to 7.1 and was stirred for 30 min. The OHAp slurry was aged for 24 h at room temperature and decanted before filtering. The filtered cake was dried at 105 °C during 12 h. The solid, previously ground in a vibratory mill, was heated at 1200 °C for 1 h. Finally, the OHAp was milled for 20 h.

2.2. OHAp characterization

The OHAp powder was characterized by X-ray diffraction (XRD), X-ray fluorescence (XRF), scanning electron microscopy (SEM), N_2 adsorption isotherm, and particle size distribution.

XRD patterns were obtained in a Philips X'Pert MPD diffractometer using CuK_α radiation in the range of 5–120° 2θ with step size of 0.02° and a time per step of 10 s. The phase quantification was made by the Rietveld method using the program X'Pert Plus. Quantitative analysis of Ca and P were performed by X-ray fluorescence on a S4 EXPLORER, Brucker AXS equipped with an Rh X-ray tube (1000 W, 50 mA). First, a calibration curve was elaborated by using seven calcium phosphate patterns with different Ca/P ratio. The correlation coefficient obtained for Ca and P were 0.999 and 0.984, respectively. The SEM study was made in a JEOL 6400 Microscope-Oxford Pentafet super ATW system; the samples were gold plated. Specific surface area was calculated from the N_2 absorption isotherm by using the BET method in a Micromeritics ASAP2010 operating between 10 and 127 kPa. Particle size distribution was measured by sedimentation in a Micromeritics Sedigraph 5100 Size Analyzer.

2.3. Suspension preparation and characterization

The suspension vehicle contained 15 wt % of methacrylamide (Aldrich) and N,N'methylenebisacrylamide (Aldrich) monomers in a 6/1 ratio. The dispersant agent for OHAp powder (Darvan 811, R.T. Vanderbilt Company, Inc.) was added to the suspension vehicle. Darvan 811 (solution of sodium polyacrylate) was used at 1.5 wt % to OHAp powder weight. The resultant solution was added to the OHAp powder and all compounds were mixed in a rotating mill for 30 min. After this time, a 10 wt % solution of ammonium persulfate (Aldrich) and a 99 wt % solution of N,N,N',N' tetramethylene diamine (Aldrich) were added as initiator and catalyst, respectively and mixed for 3 min. The concentrations of initiator and catalyst added to the suspension allowed a workable time long enough for the necessary manipulation for the casting.

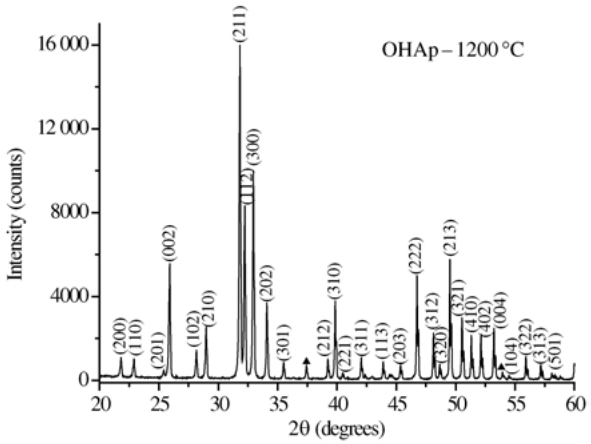

Figure 1 XRD pattern of OHAp sintered at 1200 °C (indexed). (▲) corresponds to CaO.

The suspension viscosity was measured with a Haake ReoStress RS75 rheometer with a cone-plaque system in the shear rate range of 0.1–700 s^{-1} at 20 °C.

2.4. Preparation of porous bodies

The pieces were obtained by embedding polyurethane foams with the suspension previously obtained. Four kinds of commercial polyurethane foams with different characteristics (A, B, C, and D; Polialcala S.A.) were used. The foams were soaked in the suspension contained in a polyethylene mold. More suspension was added, if required, till the saturation was reached. The molds were placed in a closed chamber and a N_2 flow was passed for 15 min. After that the closed chamber was heated at 50 °C for 2.5 h. The pieces were removed and freeze-dried for 24 h. In order to produce the burn out of the foam, the dried pieces were heated at a heating rate of 1 °C/min to 900 °C for 3 h and, finally, at 5 °C/min to 1300 °C to get the sinterization. Two dwell times (3 and 24 h) were used in order to study the influence of sintering time in the phase composition and porosity of the resulting pieces.

2.5. Characterization of porous pieces

The phase composition of the sintered pieces was quantified by DRX measurements by the Rietveld method as previously mentioned. In order to determine the residual content of the foams, elemental analysis was made in a Leco CNS-200 carbon, nitrogen and sulphur analyzer. The microstructure of the pieces was studied by SEM. The pores diameter distribution was obtained by Hg intrusion using a Micromeritics Autopore III 9420 porosimeter.

3. Results and discussion

3.1. Powder characteristics

Fig. 1 shows the XRD pattern of sintered powder at 1200 °C. Maxima indexed on the basis of an OHAp phase [24] can be observed. Two maxima at 37.4° and 53.9° 2θ could not be assigned to OHAp but were attributable to CaO [25]. The phase quantification, obtained by Rietveld method, yielded a 1.3 wt % of CaO. The Ca/P ratio

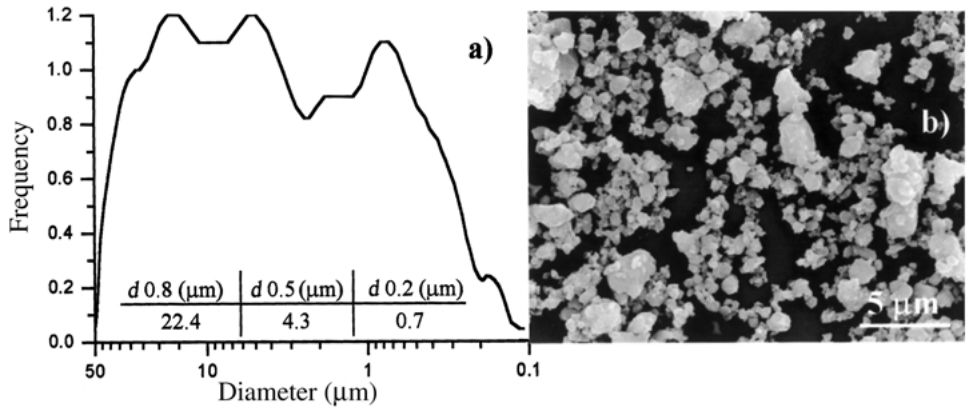

Figure 2 (a) Particle size distribution obtained by sedimentation and (b) SEM micrograph of OHAp sintered at 1200 °C.

obtained by XRF was 1.68. Specific surface area of sintered OHAp powder after milling was 3.5 m^2/g.

In Fig. 2 the particle size distribution and morphology of OHAp powder are shown. The results obtained from sedimentation showed a wide size distribution between 50 and 0.1 μm, being the average particle size 4.3 μm. By SEM it was observed that the OHAp particles showed irregular shape, with a wide distribution of particle size, but always smaller than 6 μm. The difference observed in the results, in function of the method used, could be attributed to the formation of agglomerates in the suspension when the measurement is carried out by sedimentation.

3.2. Suspension characteristics

In order to obtain pieces from gelcasting method it is necessary a solid content of at least 50% in volume, to avoid cracks formation as a consequence of the volume contraction during drying and sintering process [26]. In addition, in our case, the suspension must have a low viscosity to ensure a complete and fast absorption in the foam. To obtain slurries of low viscosity, it is necessary to use an OHAp powder with a surface area of around 10 m^2/g [27, 28] in order to avoid undesirable agglomerates that can be produced if powders with higher surface area were chosen. In addition, this surface area value would be the appropriate for the sintering process. Although powder heated at temperatures below 1200 °C had a surface area equal or lower than 10 m^2/g, the best results were obtained with OHAp powder sintered at 1200 °C.

The suspension prepared containing a 76 wt % (50V%) of OHAp sintered at 1200 °C showed a very low viscosity (0.08 Pa s), which allows the introduction of a high content of OHAp and the fast absorption of the suspension in the foam.

3.3. Characterisation of porous bodies

Polymerization of the suspensions began at 50 °C in a short time and, once the samples were removed, solid pieces perfectly conformed were obtained. After freeze-drying and sintering process, neither contraction nor cracking were observed showing the obtained pieces a good strength to be handled.

The presence of carbon and nitrogen in the porous bodies after the burn out process was not detected by elemental analysis, which indicates the complete elimination of the foam. The XRD patterns of the pieces were identical for all samples. In Fig. 3 the XRD patterns of pieces obtained from D foam after sintering at 1300 °C for 3 and 24 h, respectively, are shown. The maxima of the OHAp phase [24] can be observed. In addition, another maximum at 29.8° was observed in the sample sintered during 3 h which could be assigned to $Ca_4(PO_4)_2O$ (TTCP) [29]. In the sample sintered for 24 h additional maxima of this phase (TTCP) were observed. The presence of CaO was not detected by XRD. The phase quantification, obtained by Rietveld method yields a percentage of TTCP of 3.5 and 8.4 wt %, for the porous bodies sintered for 3 and 24 h at 1300 °C, respectively.

Fig. 4 shows the results obtained from the Hg porosimetry for all samples sintered for 3 h. In all cases (Fig. 4a), a bimodal distribution of pores with maxima centerd at ≈ 45 and 1.0 μm was observed. The distribution of pores between 100 and 10 μm is shown in Fig. 4b. As can be observed, the size of these pores depends on the foam used being the D foam the one with the higher value (55.3 μm) while the A showed the lower one (30.8 μm). On the other hand, no variation on the size of the small pores (1 μm) with the foam was observed.

Fig. 5 shows the micrographs corresponding to the pieces obtained from foams D and A sintered for 3 h at 1300 °C. It can be observed that the pieces are constituted by polyhedral-like particles surrounded by a network of

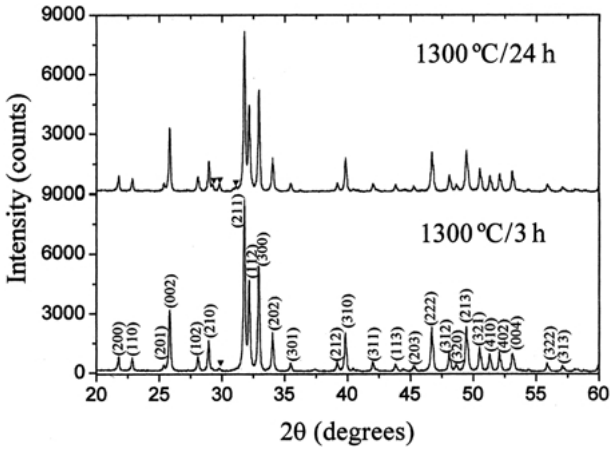

Figure 3 XRD pattern of the pieces prepared from the D foam after sintering at 1300 °C for 3 and 24 h. Indexed maxima correspond to OHAp and (▼) corresponds to $Ca_4(PO_4)_2O$.

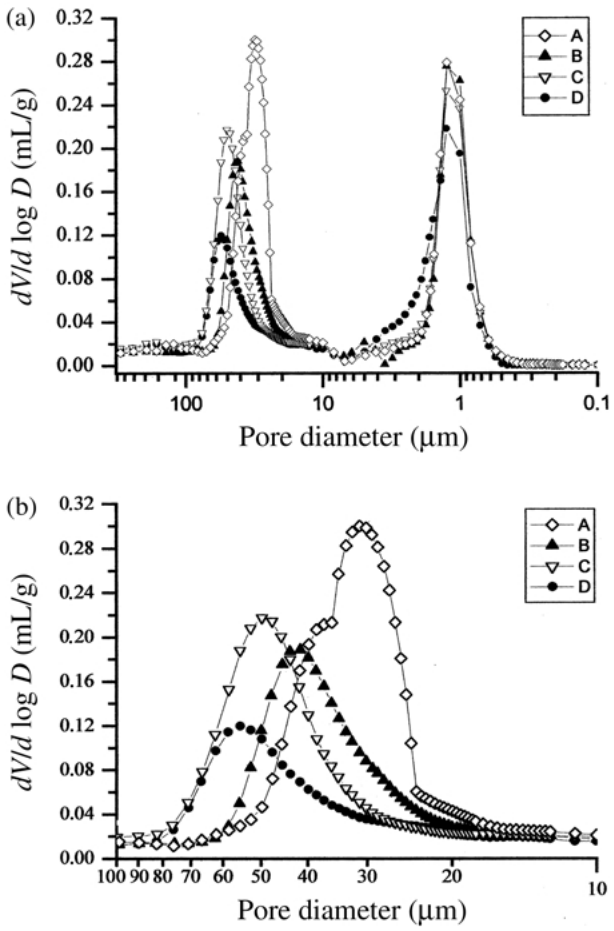

Figure 4 Pore size distribution of the pieces sintered at 1300 °C for 3 h determined by Hg porosimetry (a) from 325 to 0.1 μm and (b) from 100 to 10 μm.

pores completely interconnected. The particle size average was of 0.45 mm for the pieces obtained from the A foam and 1.0 mm for those obtained from the D foam (Fig. 5b). The porous pieces obtained from B and C foams presented intermediate values.

Since no variations in the particles size were observed as a function of the sintering time, only the micrographs of pieces sintered for 3 h are shown. The size of the particles was controled by the characteristics of the foam. The foam D presents 25 cells/cm while the A is 33 cells/cm, therefore, the cells size is higher in the D case and the particles obtained from the foam must be higher, as actually occurs. On the contrary, the cells size in the A foam is lower and the particles size is also lower. For the

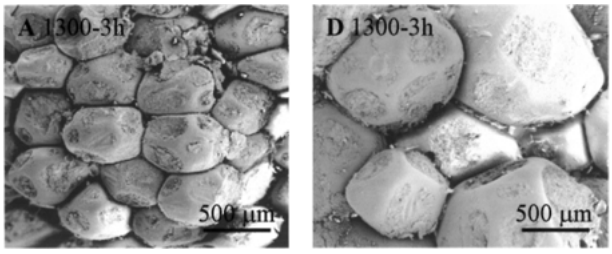

Figure 5 SEM micrographs of the pieces sintered at 1300 °C for 3 h prepared from the foams A and D (Magnification × 50).

porous pieces prepared from B and C that presents 28 cells/cm, intermediate values were obtained.

In Fig. 6 the micrographs of the macropores, previously detected by Hg porosimetry, for the pieces obtained from A and D foams are shown. It can be observed the higher pore size for the pieces obtained from the D foam. The presence of small pores (≈ 1 μm) on the surface of the particles is shown in the magnification X1000. The size of the pores observed by SEM agrees with the ones obtained from Hg porosimetry.

Fig. 7 shows the pore size distribution for all the pieces obtained sintered for 3 and 24 h. In all cases, the higher the sintering times, the lower the fraction of pores of 1 μm. This could be explained considering that the sinterization process takes place between the small crystallites of OHAp that form the particles. In general, it can be observed a small displacement to higher values for the pores of higher size when the sintering time increases. This could be due to the small contraction of the particles during the sinterization process, which would produce an increase of the interparticle pores.

The interconnected pores network among the particles is formed by the loss of the foam. The higher the number of cells/cm of the foam, the lower the thickness of the cells wall. This is the reason why the pores size is 30.8–34.7 μm for the pieces obtained from the A foam (33 cells/cm) while in the ones obtained from the D foam (25 cells/cm) is 55.3–58.6 μm.

4. Conclusions

Porous machinable pieces of OHAp have been prepared from polyurethane foams by combination of gelcasting and burn out methods. The pieces are constituted by polyhedral-like particles with an average size of 0.45–1.0 mm that are surrounded by an interconnected

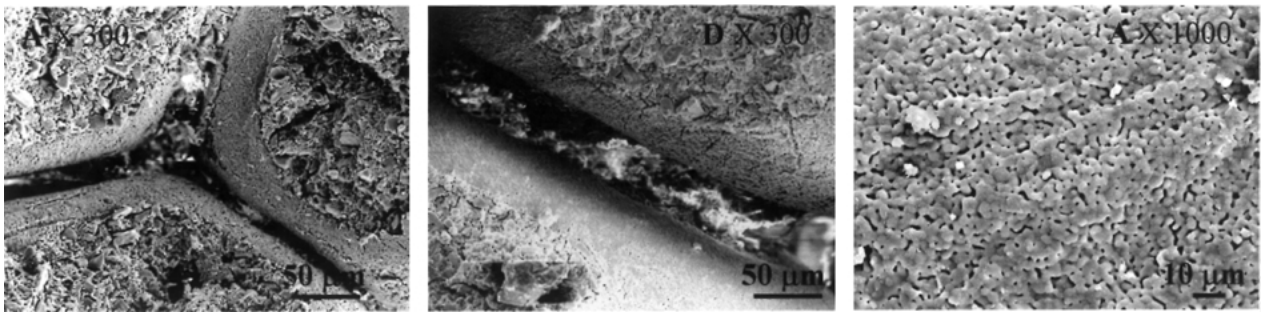

Figure 6 SEM micrographs of the pieces sintered at 1300 °C for 3 h prepared from the foams A and D (Magnification × 300) and A (Magnification × 1000).

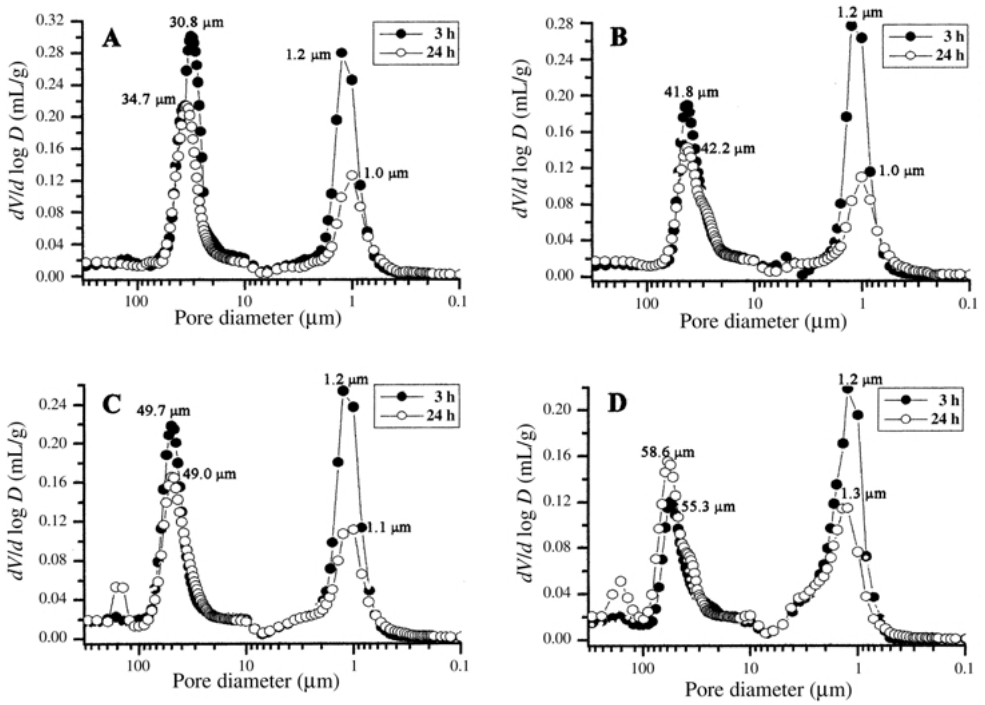

Figure 7 Pore size distribution of the pieces obtained from the foams A, B, C, and D sintered at 1300 °C for 3 and 24 h determined by Hg porosimetry.

network of pores. The porous pieces showed a bimodal distribution of the pores size between 30.8–58.6 µm and ≈ 1.0 µm. The size of the interconnected pores (30.8–58.6 µm) can be controled as a function of the cells in the used foam. The composition of the ceramics and the volume of the small pores on the particles surface can be modified as a function of the sintering time. The presence of pores could promote the bone ingrowth and also could be used to insert different drugs, which makes these porous pieces a potential candidate to be used as non-load-bearing bone implants and as drug delivery systems.

Acknowledgment

Financial support of CICYT, Spain, through research projects MAT99-0461 and ICI-MEC/PR264/97 are acknowledged. Authors also thank A. Rodríguez (C.A.I. electron microscopy, UCM), F. Conde and E. Fraga (C.A.I. X-ray diffraction, UCM) for valuable technical and professional assistance. F. López-Díaz (Polialcalá S.A) supplied the polyurethane foams kindly.

References

1. H. AOKI, in ''Science and Medical Applications of Hydroxyapatite'' (Takayama Press System Center Co., Tokyo, 1991) p. 1.
2. L. L. HENCH, *J. Am. Ceram. Soc.* **81** (1993) 1705.
3. K. DE GROOT, *Ceram. Int.* **19** (1993) 363.
4. C. REY, in ''Calcium Phosphates in Biological and Industrial Systems'' (Kluwer Academic Publishers, London, 1998) p. 217.
5. F. B. BAGAMBISA, U. JOOS and W. SCHILLI, *J. Biomed. Mater. Res.* **27** (1993) 1047.
6. E. TSURUGA, H. TAKITA, H. ITOH, Y. WAKISAKA and Y. KUBOKI, *J. Biochem.* **121** (1997) 317.
7. J. J. KLAWITTER and S. F. HULBERT, *J. Biomed. Mater. Res.* **5** (1971) 161.
8. S. F. HULBERT, J. S. MORRISON and J. J. KLAWITTER, *ibid.* **6** (1972) 347.
9. B.-S. CHANG, C.-K. LEE, K.-S. HONG, H.-J. YOUN, H.-S. RYU, S.-S. CHUNG and K.-W. PARK, *Biomaterials* **21** (2000) 1291.
10. K. A. HING, S. M. BEST, K. E. TANNER, W. BONFIELD and P. A. REVELL, *J. Mater. Sci.: Mater. Med.* **10** (1999) 663.
11. N. TAMAI, A. MYOUI, T. TOMITA, T. NAKASE, J. TANAKA, T. OCHI and H. YOSHIKAWA, *J. Biomed. Mater. Res.* **59** (2002) 110.
12. D. M. ROY and K. LINNEHAN, *Nature* **247** (1974) 220.
13. D.-M. LIU, *J. Mater. Sci. Lett.* **15** (1996) 419.
14. J. BOULER, M. TRECANT, J. DELECRIN, J. ROYER, N. PASSUTI and G. DACULSI, *J. Biomed. Mater. Res.* **32** (1996) 603.
15. E. TSURUGA, H. TAKITA, H. ITOH, Y. WAKISAKA and Y. KUBOKI, *J. Biochem* **121** (1997) 317.
16. P. SEPULVEDA, J. G. P. BINNER, S. O. ROGERO, O. Z. HIGA and J. C. BRESSIANI, *J. Biomed. Mater. Res.* **50** (2000) 27.
17. A. TAMPIERI, G. CELOTTI, S. SPRIO, A. DELCOGLIANO and S. FRANZESE, *Biomaterials* **22** (2001) 1365.
18. T.-M. G. CHU, J. W. HALLORAN, J. HOLLISTER and S. E. FEINBERG, *J. Mater. Sci.: Mater. Med.* **12** (2001) 471.
19. L. M. RODRIGUEZ-LORENZO, M. VALLET-REGI and J. M. F. FERREIRA, *J. Biomed. Mater. Res.* **60** (2002) 232.
20. X. YANG and Z. WANG, *J. Mater. Chem.* **8** (1998) 2233.
21. J. TIAN and J. TIAN, *J. Mater. Sci.* **36** (2001) 3061.
22. M. A. JANNEY, US Pat. 4894 194 (1990).
23. A. C. YOUNG, O. O. OMATETE, M. A. JANNEY and P. A. MENCHHOFER, *J. Am. Ceram. Soc.* **74** (1991) 612.
24. Powder Diffraction File, No. 9-432. Data base sets 1–49 plus 70–86. International center for Diffraction Data (1999).
25. Powder Diffraction File, No. 43-1001. Data base sets 1–49 plus 70–86. International center for Diffraction Data (1999).
26. M. A. JANNEY, O. O. OMATETE, C. A. WALLS, S. D. NUNN, J. R. OGLE and G. WESTMORELAND, *J. Am. Ceram. Soc.* **81** (1998) 581.
27. F. LELIEVRE, D. BERNACHE-ASSOLLANT and T. CHARTIER, *J. Mater. Sci.: Mater. Med.* **7** (1996) 489.
28. L. M. RODRIGUEZ-LORENZO, M. VALLET-REGI and J. M. F. FERREIRA, *Biomaterials* **22** (2001) 1847.
29. Powder Diffraction File, No. 25-1137. Data base sets 1–49 plus 70–86. International center for Diffraction Data (1999).

Received 24 May
and accepted 27 June 2002